

Spectral wave dissipation over a barrier reef

Ryan J. Lowe,¹ James L. Falter,² Marion D. Bandet,³ Geno Pawlak,³ Marlin J. Atkinson,² Stephen G. Monismith,¹ and Jeffrey R. Koseff¹

Received 12 September 2004; revised 20 November 2004; accepted 1 February 2005; published 5 April 2005.

[1] A 2 week field experiment was conducted to measure surface wave dissipation on a barrier reef at Kaneohe Bay, Oahu, Hawaii. Wave heights and velocities were measured at several locations on the fore reef and the reef flat, which were used to estimate rates of dissipation by wave breaking and bottom friction. Dissipation on the reef flat was found to be dominated by friction at rates that are significantly larger than those typically observed at sandy beach sites. This is attributed to the rough surface generated by the reef organisms, which makes the reef highly efficient at dissipating energy by bottom friction. Results were compared to a spectral wave friction model, which showed that the variation in frictional dissipation among the different frequency components could be described using a single hydraulic roughness length scale. Surveys of the bottom roughness conducted on the reef flat showed that this hydraulic roughness length was comparable to the physical roughness measured at this site. On the fore reef, dissipation was due to the combined effect of frictional dissipation and wave breaking. However, in this region the magnitude of dissipation by bottom friction was comparable to wave breaking, despite the existence of a well-defined surf zone there. Under typical wave conditions the bulk of the total wave energy incident on Kaneohe Bay is dissipated by bottom friction, not wave breaking, as is often assumed for sandy beach sites and other coral reefs.

Citation: Lowe, R. J., J. L. Falter, M. D. Bandet, G. Pawlak, M. J. Atkinson, S. G. Monismith, and J. R. Koseff (2005), Spectral wave dissipation over a barrier reef, *J. Geophys. Res.*, 110, C04001, doi:10.1029/2004JC002711.

1. Introduction

[2] Coral reefs are abundant in shallow tropical and subtropical coastal regions, environments where significant amounts of surface wave energy can be dissipated through wave breaking and bottom friction processes. The physical structure of coral reefs is notably different from that of beaches, which to date have been the primary focus of nearshore hydrodynamic studies [Komar, 1998]. Unlike beaches, which typically have mild slopes and relatively smooth bottoms, coral reefs often form a steep transition from relatively deep to shallow water, and generate a very rough bottom surface due to the presence of reef organisms [Wiens, 1962].

[3] Accurately predicting surface waves on coral reefs is important for several reasons. First, as waves break on a reef they produce an increase in the mean water surface elevation, creating a pressure (radiation stress) gradient that drives reef circulation [Longuet-Higgins and Stewart, 1962]. These wave-driven currents are responsible for the cross-reef transport of nutrients, sediment, plankton, larvae,

etc., and accordingly their prediction has been the focus of several analytical and numerical studies [e.g., Symonds *et al.*, 1995; Hearn, 1999; Kraines *et al.*, 1999; Tartinville and Rancher, 2000].

[4] Second, wave processes on coral reefs play a major role in determining coral reef ecology. Wave-induced forces can have a detrimental effect by destroying delicate reef organisms. Wave exposure is thus often used as a predictor of the community structure of coral reefs [e.g., Dollar, 1982; Dollar and Tribble, 1993; Grigg, 1998]. Alternatively, there is increasing evidence that water motion can benefit coral reef organisms by increasing the rate at which these organisms take up nutrients and hence their overall productivity. Several studies have found that under unidirectional flow, nutrient uptake by coral reef communities is positively correlated with bed shear stress at a rate that can be predicted using engineering mass transfer formulas [e.g., Atkinson and Bilger, 1992; Baird and Atkinson, 1997; Thomas and Atkinson, 1997]. However, many coral reefs are found in coastal regions with significant wave activity such that wave-induced shear stresses exerted on the bed can often be much larger than the stress attributed to the unidirectional current. This enhanced wave stress can increase the rate of nutrient uptake [e.g., Falter *et al.*, 2004]. Hearn *et al.* [2001] proposed a model that predicts these uptake rates as a function of the rate at which wave energy is dissipated by bottom friction. Thus the development of an accurate approach for parameterizing wave dissipation processes on coral reefs is needed to understand and model the productivity and distribution of reef organisms.

¹Environmental Fluid Mechanics Laboratory, Stanford University, Stanford, California, USA.

²Hawaii Institute of Marine Biology, University of Hawaii, Kaneohe, Hawaii, USA.

³Department of Oceans and Resources Engineering, University of Hawaii, Honolulu, Hawaii, USA.

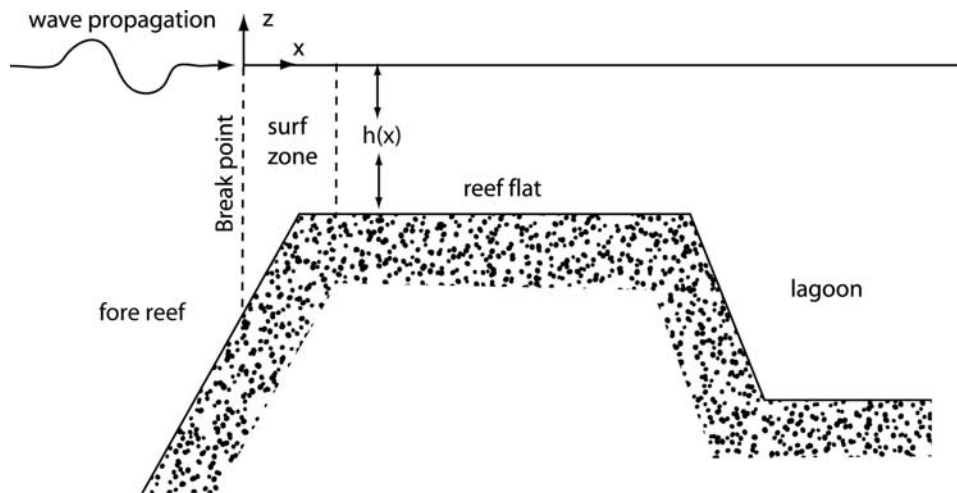


Figure 1. Cross section of a barrier reef and lagoon.

[5] The geomorphology of a typical barrier reef is divided into three main regions (Figure 1): (1) a sloping fore reef, (2) a reef flat where the bottom slope is minimal, and (3) a deep lagoon [Wiens, 1962]. As waves propagate over the reef they undergo several transformations. Waves first begin to interact with the fore reef when their wavelength becomes comparable to the local water depth h . As they move shoreward and shoal, the waves increase in height while dissipating some of their energy to bottom friction. Eventually their height becomes some critical fraction of the water depth and the waves become unstable and break. At a given cross-reef location, a maximum allowable wave height thus exists that is controlled by the local water depth according to

$$H_{\text{rms}} < \gamma h, \quad (1)$$

where H_{rms} is the root-mean-squared (RMS) wave height and γ is a critical breaking parameter [Thornton and Guza, 1982]. This breaking region extends a finite distance, denoted as the surf zone in Figure 1, and in this region a significant amount of the incident wave energy can be dissipated through breaking. On sandy beaches, wave energy dissipation is predominantly due to breaking [e.g., Thornton and Guza, 1983] and for many coral reefs wave breaking has been assumed to be the primary source of dissipation [e.g., Young, 1989; Gourlay, 1994; Massel and Gourlay, 2000].

[6] Unlike beaches where the water depth approaches zero toward shore, the water depth over the reef flat is nonzero and relatively constant. Waves with height ratios that are smaller than the critical breaking limit γ in equation (1) are then free to pass onto the reef flat. The barrier reef thus serves as a low-pass wave height filter by filtering out waves with heights larger than the depth-limited maximum. For most barrier reefs the reef flat is quite shallow, usually no deeper than a few meters, so waves propagating across the reef flat can dissipate significant amounts of energy to bottom friction. Moreover, coral reef organisms are known to form some of the roughest surfaces in the coastal ocean, so frictional dissipation rates can be expected to be larger than sandy or even rocky reef sites located along the continental shelf.

[7] A limited number of field experiments have investigated wave transformation over coral reefs. These include studies of fringing reefs, which are attached to the shoreline [e.g., Lee and Black, 1979; Gerritsen, 1981; Brander et al., 2004], as well as barrier reefs where a lagoon exists on the leeward side of the reef [e.g., Young, 1989; Hardy and Young, 1996; Lugo-Fernandez et al., 1998a, 1998b]. Perhaps the most comprehensive field study conducted on a barrier reef is that described by Hardy and Young [1996], where wave heights at four stations at a site on the Great Barrier Reef were recorded for a 3 week period. The study confirmed the existence of a maximum stable wave height on the reef flat which is controlled by the reef flat water depth and is modulated by the tidal elevation.

[8] A major challenge for modeling wave transformation on coral reefs is choosing an appropriate parameterization for wave dissipation due to wave breaking and bottom friction. Several formulas exist to predict rates of wave dissipation, but these are semiempirical and must be calibrated through experiments. While the studies cited above include detailed observations of wave attenuation across reefs, the focus of these studies was not on calculating rates of wave energy dissipation, or more specifically isolating the relative contributions of wave breaking and bottom friction. Measuring dissipation due to wave breaking is particularly difficult since for spectral wave conditions, the case where the wave field is composed of an infinite number of frequency components, the width of the surf zone is difficult to define [Hardy and Young, 1996]. As a consequence, measurements of the rate of wave breaking dissipation on reefs have been confined to controlled laboratory experiments such as those reported by Gourlay [1994]. Measuring rates of frictional wave dissipation in the field is similarly difficult, but some estimates have been reported by Gerritsen [1981], Nelson [1996], and Falter et al. [2004].

[9] In this paper we describe results from a field experiment where wave transformation across a barrier reef in Kaneohe Bay, Oahu, Hawaii was measured. Wave energy dissipation was estimated by determining the decrease in wave energy flux at several sites across the reef. A goal of this study was to isolate the relative contributions of wave breaking and frictional dissipation from the total incident

wave energy dissipated on the reef. In addition, special attention is given to parameterizing bottom friction, which is particularly important over coral reefs. Frictional dissipation was investigated using dissipation measurements on the reef flat, since breaking does not occur within this region. The spectral wave friction model developed by *Madsen et al.* [1988] was used to investigate how wave energy is dissipated among the different frequency components. This model has been validated in laboratory experiments by *Mathisen and Madsen* [1999], but has yet to be applied to field data sets, in part because frictional dissipation is often difficult to accurately measure in the field environment. The reef flat at Kaneohe Bay is ideal for this investigation since waves propagate across the reef flat maintaining a relatively constant direction with minimal refraction such that the problem can be treated as one-dimensional. Moreover, the reef flat is both shallow and very rough, so the frictional dissipation signal is strong, making it well suited for this type of study. Finally, in this study a comparison is made between the hydraulic roughness obtained from the frictional dissipation measurements and the surveyed physical bottom roughness. Data collected from previous laboratory studies have been used to develop empirical formulas describing frictional dissipation as a function of wave kinematics and the physical roughness properties. In principle, it should be possible to apply these formulas to coral reef sites, however to date no studies have specifically linked the measured bottom roughness of a coral reef to observed rates of frictional dissipation.

[10] This paper is organized as follows. In section 2, an overview of theory which can be used to describe wave transformation on coral reefs is presented. A description of the field site and experimental setup is presented in section 3, including a summary of the wave and tide conditions encountered in the experiments. Results from the experiments are described in section 4. In this section, measurements of wave height attenuation across the reef are used to estimate rates of dissipation, and the *Madsen et al.* [1988] spectral wave friction model is used to investigate frictional dissipation measured on the reef flat. The hydraulic roughness calculated from the frictional dissipation measurements is then compared to direct measures of the physical bottom roughness obtained from surveys. Finally, wave breaking dissipation on the fore reef is investigated using a simple one-dimensional numerical model.

2. Spectral Wave Dissipation

[11] Wave energy dissipation on the barrier reef at Kaneohe Bay is assumed to be dominated by wave breaking and bottom friction. Wave models generally parameterize dissipation using the wave energy conservation equation. For spectral wave conditions, the continuous wave spectrum is typically discretized into a total of N discrete frequency components of index j . For the case where waves of all frequency components propagate in the same direction x , the one-dimensional wave energy equation is

$$\frac{\partial F_j}{\partial x} = -\epsilon_{b,j} - \epsilon_{f,j} \quad (2)$$

$$F_j = E_j C_{g,j}, \quad (3)$$

where for each j th frequency component, F_j is the wave energy flux, E_j is the wave energy density, $C_{g,j}$ is the group velocity, and $\epsilon_{b,j}$ and $\epsilon_{f,j}$ represent the rates of energy dissipation (per unit area) due to wave breaking and bottom friction, respectively. It should be noted that equation (2) does not include the potential transfer of energy between the different frequency components due to nonlinear interactions, as described by *Hasselmann* [1962]. This issue will be discussed further in section 4. By applying linear wave theory, the energy density and group velocity are

$$E_j = \frac{1}{2} \rho g a_j^2 \quad (4)$$

$$C_{g,j} = \frac{1}{2} \left(1 + \frac{2k_j h}{\sinh 2k_j h} \right) \frac{\omega_j}{k_j}, \quad (5)$$

respectively, where for the j th component, ω_j is the radian frequency, k_j is the wave number and a_j is the wave amplitude. In this formulation the effect of a background current has not been included in equation (3), since measured currents on the Kaneohe reef during the experiment were very weak. Cross-reef currents U were measured to be at most 4 cm/s, so their effect can be neglected since $Uk_j/\omega_j < 0.01$ for all frequency components included in the analysis [*Dean and Dalrymple*, 1991].

[12] Several semiempirical models have been developed to predict the dissipation functions $\epsilon_{b,j}$ and $\epsilon_{f,j}$ in equation (2). These models have been validated in laboratory and field experiments. Owing to the limited number of field measurements on coral reefs, and because the bottom slopes of reefs can be very steep and the bottom roughness can be large, the application of these models to coral reefs has been questioned by *Massel and Gourlay* [2000]. A summary of some of the models used to predict wave dissipation follows.

2.1. Dissipation Due to Wave Breaking

[13] Because wave breaking is a highly nonlinear process, models which predict wave breaking dissipation are generally semiempirical. For the most part, these models have been derived for coastlines where the bottom slope is mild [e.g., *Battjes and Janssen*, 1979; *Dally et al.*, 1985; *Thornton and Guza*, 1983]. An often cited model is that of *Thornton and Guza* [1983], which parameterizes the rate of bottom friction for spectral wave conditions according to

$$E_b = \frac{3\sqrt{\pi}}{16} \frac{\rho g f_p B^3}{\gamma^4 h^5} H_{\text{rms}}^7, \quad (6)$$

where E_b represents the rate of change of the total wave energy due to breaking summed over all of the frequency components, i.e., $E_b = \sum_{j=1}^N \epsilon_{b,j}$. Here f_p is the peak frequency in the wave energy spectrum, γ is the critical wave breaking parameter (equation (1)), B is an empirical constant of order 1, and H_{rms} is the RMS wave height defined later in section 4. Owing to the fact that E_b represents the total rate of dissipation (i.e., the sum over all frequencies), equation (6) has been applied to spectral wave conditions by assuming that the rate of dissipation in each frequency component is proportional to the wave height of that component [e.g., *Chawla et al.*, 1998].

[14] The dissipation function in equation (6) has been validated for mild bottom slopes. However, for some reefs the bottom slope can be very steep and *Massel and Gourlay* [2000] propose an alternative form of E_b , based on a modification of the model by *Battjes and Janssen* [1979]. Given that the barrier reef at Kaneohe Bay is unusually wide (~ 2 km) and hence the bottom slope is relatively mild ($\sim 1:50$), which places it within the stated applicability limits of the model, equation (6) will be used in this paper to model wave breaking dissipation.

2.2. Dissipation Due to Bottom Friction

[15] Several models have been developed to predict the rate of energy dissipation due to friction in turbulent wave boundary layer flows [e.g., *Putman and Johnson*, 1949; *Kajiura*, 1968; *Jonsson*, 1966]. These models were originally developed for monochromatic waves. *Madsen et al.* [1988] and *Madsen* [1994] extended theory originally developed for monochromatic waves to spectral wave conditions by defining representative flow parameters that are based on taking a weighted average of the given parameter by placing more weight on the frequency components that contain more wave energy. A representative maximum near-bed horizontal orbital velocity $u_{b,r}$ can thus be defined as

$$u_{b,r} = \sqrt{\sum_{j=1}^N u_{b,j}^2}, \quad (7)$$

where $u_{b,j}$ is the velocity corresponding to the j th frequency component. A representative wave radian frequency, ω_r , can similarly be defined as

$$\omega_r = \frac{\sum_{j=1}^N \omega_j u_{b,j}^2}{\sum_{j=1}^N u_{b,j}^2}. \quad (8)$$

Using the representative wave parameters in equations (7) and (8), *Madsen* [1994] showed that the rate of dissipation due to bottom friction for a given wave frequency can be modeled as

$$\epsilon_{f,j} = \frac{1}{4} \rho f_{e,j} u_{b,r} u_{b,j}^2, \quad (9)$$

where $f_{e,j}$ is the j th component of the “energy dissipation factor.” The form of dissipation in equation (9) is notable, in that it allows for wave energy to be dissipated at different rates among the different frequency components.

[16] *Madsen* [1994] further showed that for spectral waves the energy dissipation factor $f_{e,j}$ can be related to the “wave friction factor” $f_{w,j}$ according to

$$f_{e,j} = \sqrt{f_{w,r}} \sqrt{f_{w,j}} \cos \phi_j, \quad (10)$$

where $f_{w,j}$ is the j th component of the wave friction factor, $f_{w,r}$ is the representative wave friction factor, and ϕ_j is the phase angle between the bottom shear stress and the near-bed horizontal orbital velocity. The representative wave

friction factor $f_{w,r}$ in equation (10) is used to parameterize the shear stress exerted on the bed as

$$\tau_{w,r} = \frac{1}{2} \rho f_{w,r} u_{b,r}^2, \quad (11)$$

where $\tau_{w,r}$ is the representative shear stress. Several empirical formulas have been developed to predict wave friction factors as a function of the wave conditions and bottom roughness properties, and these formulas will be discussed below. Finally, by using equation (10) to estimate $f_{e,j}$, a representative energy dissipation factor $f_{e,r}$ can be determined using the weighted average approach:

$$f_{e,r} = \frac{\sum_{j=1}^N f_{e,j} u_{b,j}^2}{\sum_{j=1}^N u_{b,j}^2}, \quad (12)$$

which gives a single energy dissipation factor that is representative of the spectral wave conditions.

[17] In order to predict frictional energy dissipation $\epsilon_{f,j}$ at a given field site using equations (7)–(12), it is necessary to choose values for the wave friction factor $f_{w,j}$ and phase lag ϕ_j by somehow relating these quantities to the bottom roughness properties. For monochromatic waves, several empirical formulas exist to predict wave friction factors f_w and phase lags ϕ as a function of wave parameters and a representative hydraulic roughness length scale k_w . *Madsen* [1994] assumed that these monochromatic friction formulas can be extended to spectral waves by simply applying these formulas to each frequency component. An inherent assumption of this approach is that k_w is a constant and, hence, independent of the hydrodynamics. This assumption was found to be valid in laboratory experiments by *Mathisen and Madsen* [1999], but has yet to be directly investigated in field experiments.

[18] A number of formulas have been developed to predict wave friction factors under monochromatic wave conditions. For rough turbulent wave boundary layers, many of these formulas parameterize the wave friction factor as a function of the ratio of the near-bed horizontal wave orbital excursion amplitude $A_b = u_b/\omega$ to a hydraulic roughness length k_w [e.g., *Jonsson*, 1966; *Swart*, 1974; *Madsen*, 1994]. Although several formulas exist, *Nielsen* [1992] gives a comprehensive formula to predict wave friction factors as a function of the physical bottom roughness, by compiling data from several laboratory experiments where the bottom roughness was measured and hence was known. *Madsen* [1994] showed that these monochromatic friction formulas can be extended to spectral conditions according to

$$f_{w,j} = \exp \left[a_1 \left(\frac{u_{b,r}}{k_w \omega_j} \right)^{a_2} + a_3 \right], \quad (13)$$

where a_1 , a_2 , and a_3 are empirical coefficients given in the monochromatic friction formulas. In *Nielsen's* [1992] formula these coefficients are $a_1 = 5.5$, $a_2 = -0.2$, and $a_3 = -6.3$. Although the coefficients given by *Madsen* [1994] could alternatively be used in equation (13), we have chosen to use *Nielsen's* coefficients because he explicitly

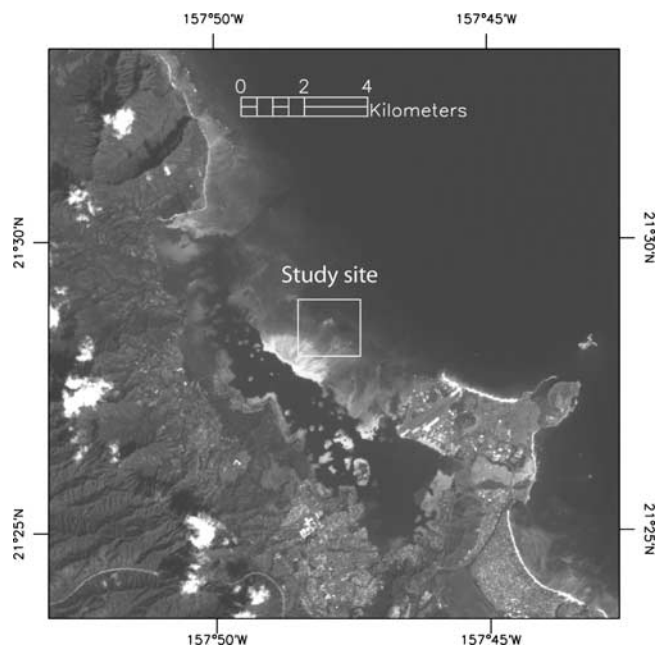


Figure 2. Kaneohe Bay, Oahu, Hawaii. The box approximately indicates the study area shown in Figure 3. (Landsat 7–ETM+ image). See color version of this figure in the HTML.

describes how to calculate k_w based on the measured bottom roughness. Use of the *Nielsen* [1992] relationship therefore allows us to compare our estimates of $f_{w,j}$, derived later from measured wave energy fluxes, with estimates of k_w based on in situ measurements of the bottom roughness.

[19] Finally, to estimate the energy dissipation factor $f_{e,j}$ using equation (10) requires an estimate of the phase angle ϕ_j for the different frequency components. *Madsen* [1994] states that the phase angle can be approximated in degrees as

$$\phi_j = 33 - 6.0 \log_{10} \left(\frac{u_{bm,r}}{k_w \omega_j} \right). \quad (14)$$

For a given $f_{e,r}$, a representative wave friction factor $f_{w,r}$ can be determined by applying equation (10) according to

$$f_{e,r} = f_{w,r} \cos \phi_r, \quad (15)$$

where the representative phase lag ϕ_r can be determined by substituting ω_r in equation (14) for ω_j .

3. Experimental Setup and Conditions

3.1. Study Site

[20] A 2 week experiment was conducted on the barrier reef in Kaneohe Bay, which is located on the northeastern (windward) shore of the island of Oahu in Hawaii (21°29'N, 157°48'W). It represents the largest sheltered body of water in the Hawaiian Islands, and extends about 15 km along shore and is approximately 3 km wide. The aerial photograph in Figure 2 shows that the Kaneohe Bay reef has a similar form to the idealized barrier reef in Figure 1. The barrier reef itself runs NW to SE along the seaward side of

the bay and is approximately 2 km wide and 10 km long. Compared to other reefs around the world, the reef at Kaneohe Bay is unusually wide, as many reefs tend to be on the order of only several hundred meters wide [*Wiens*, 1962], such as those sites described by *Hardy and Young* [1996] and *Lugo-Fernandez et al.* [1998a, 1998b]. The depth of the reef flat ranges from 3 m in the region closest to the fore reef to <1 m in the region nearest to the lagoon. Located behind the reef is a lagoon having a width 1–2 km and a depth of 10–15 m.

[21] Kaneohe Bay is exposed to the trade winds which blow most of the year from E to NE, averaging approximately 5 m/s. The wave environment is predominantly derived from two major sources: (1) wind waves derived from the trade winds with 6–10 s periods, which dominate during the summer months and (2) ocean swells 10–14 s in period that are generated by North Pacific storms primarily in the winter months. The mean tidal range in Kaneohe Bay is approximately 0.7 m with a maximum of about 1.1 m.

3.2. Instrument Deployment

[22] The instruments that were used to estimate wave dissipation were located at five sites arranged in a line oriented in the cross-reef direction (Figure 3). A summary of the instrument locations and settings is given in Table 1. Site 1 was located on the fore reef at a position such that no wave breaking would occur offshore of this site. During the experiment, the surf zone was located between sites 1 and 2. Sites 2 through 5 were located on the reef flat at least one hundred meters shoreward of where the surf zone ended. As a consequence, wave breaking was negligible between these sites.

[23] A RD Instruments 1200 kHz acoustic Doppler current profiler (ADCP) was located on the fore reef at site 1 in approximately 7 m of water, and was primarily used to measure incident wave energy flux (before breaking) and wave direction. The instrument was programmed in mode 12 (RDI's fast-pinging rate mode) to sample velocities and pressure at 1 Hz using 23 0.25 m bins. The ADCP at site 1 sampled continuously from 19 August to 3 September 2003.

[24] Site 2 was located approximately 700 m shoreward of site 1, and was the first site on the reef flat. All sites on the reef flat (sites 2–5) were spaced approximately 100 m apart. A sawhorse instrument frame of length 1.5 m and height 1.0 m was located at site 2 in approximately 2 m of water. The frame was situated such that the support beam was normal to the wave propagation direction to minimize flow interference by the frame legs. Two Nortek Vector acoustic Doppler velocimeters (ADV) were mounted to the instrument frame. The upper ADV sampled velocities 1.3 m above the bed while the lower ADV sampled 0.3 m above the bed. Each ADV sampled velocities and pressure at 16 Hz, and was operated in burst mode collecting 20 min bursts every hour (19200 samples per burst). The memory and battery endurance for these sampling parameters was only 7 days, so the two ADVs were retrieved and redeployed with a 10 hour turn around time on 27 August. Seabird Electronics 26 pressure sensors were placed at sites 3–5 to measure wave heights across the reef flat. Each sampled pressure at 2 Hz in 17 min bursts (2048 samples per

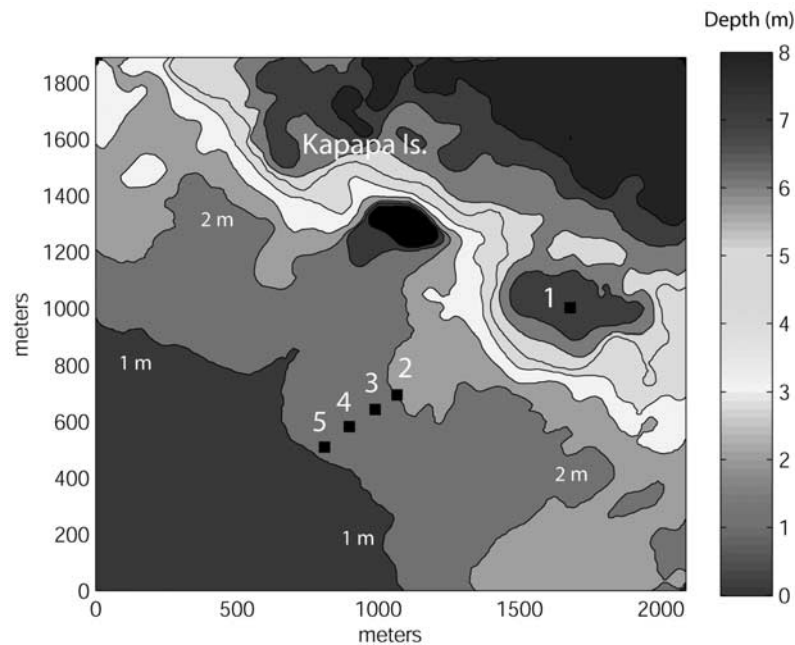


Figure 3. Reef bathymetry and instrument locations. Water depth is based on the mean tidal elevation during the experiment. The contour interval is 1 m, and the 1 and 2 m isobaths are highlighted. Instrument locations are indicated by the squares. See color version of this figure in the HTML.

burst) every hour. Finally, an offshore directional wave buoy (Datawell, Netherlands) was located approximately 15 km southeast of Kaneohe Bay ($21^{\circ}24.9'N$, $157^{\circ}40.7'W$), which recorded wave conditions every 30 min.

3.3. Wave and Tide Conditions

[25] The experiment was conducted from 18 August to 4 September 2003. During the experiment the incident waves measured by the offshore wave buoy were predominantly trade wind generated with a peak period T_p between 7 and 10 s (Figure 4). During the beginning of the experiment, strong trade winds in the eastern Pacific generated waves with a RMS wave height $H_{rms} \approx 1.5$ m

propagating westward (toward 270°). Beginning on day 238 the trade winds weakened and the wave height decreased to as low as $H_{rms} \approx 0.7$ m. The peak direction at this time switched to roughly 180° (toward the south). Finally, near day 245, Hurricane Jimena passed just south of the Hawaiian Islands and generated waves with $H_{rms} \approx 2.2$ m, which is unusually large for this time of year, and is more typical of winter swell wave heights. A wide range of wave conditions were thus encountered over this relatively short experiment. An analysis of wave heights measured at the same wave buoy for the 3 year period from 1 January 2001 to 31 December 2003 showed that this range of wave heights ($H_{rms} = 0.7\text{--}2.2$ m) occurred

Table 1. Instrument Locations and Settings

Instrument(s)	Settings
Datawell directional wave buoy	<i>Offshore</i> data recorded every 30 min
RDI 1200 KHz ADCP (with pressure sensor)	<i>Site 1</i> operated in mode 12 bin size = 0.25 m total bins = 23 16 subpings at 25 Hz ping rate = 1 Hz
Two Nortek Vector ADVs (with pressure sensors)	<i>Site 2</i> 16 Hz sampling rate operated in burst mode 19200 samples per burst one burst every hour
Seabord Electronics 26 pressure sensors	<i>Sites 3–5</i> 2 Hz sampling rate operated in burst mode 2048 samples per burst one burst every hour

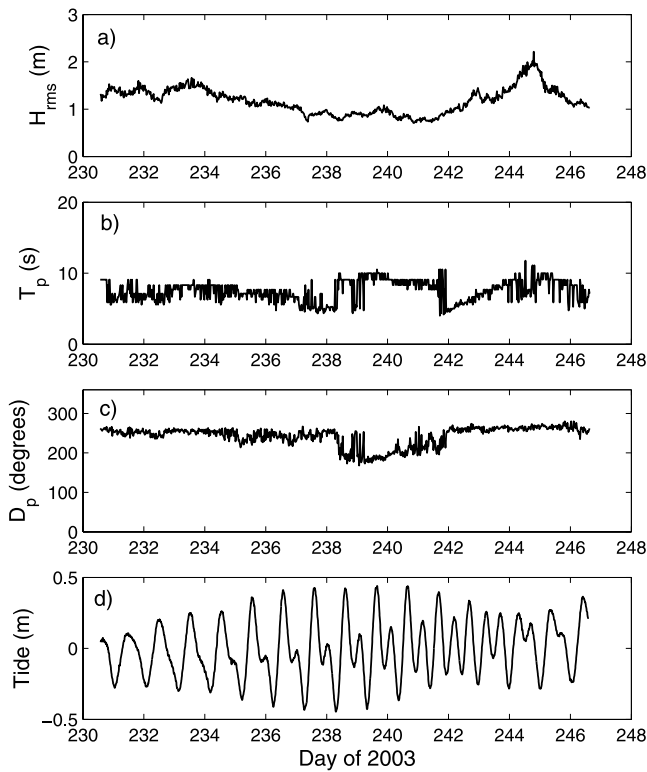


Figure 4. Wave and tide conditions. (a) Offshore RMS wave height H_{rms} . (b) Offshore peak period T_p . (c) Offshore dominant wave direction D_p . (d) Tidal elevation (as represented by the deviation from mean depth measured at site 2).

greater than 95% of the time. Thus the experiments incorporated the vast majority of the historical wave height conditions.

[26] Finally, tide data recorded on the reef flat at site 2 is shown in Figure 4d. The experiment covered a complete spring neap tidal cycle.

4. Observations and Results

4.1. Wave Heights

[27] Waves propagating across the reef dissipate energy through wave breaking and bottom friction. According to the wave energy equation (equation (2)), a decrease in the wave energy flux will be accompanied by a change in wave height across the reef. Owing to the relatively mild slope of the fore reef ($\sim 1:50$) wave reflection, as estimated using the *Battjes* [1974] sloping bottom reflection formula, is extremely small and can be neglected. We therefore used wave height attenuation measurements to estimate wave dissipation.

[28] Wave height variation across the reef was measured using the pressure time series measurements at sites 1–5. The spectral density of the water surface elevation S was calculated for each hourly burst by first calculating the one-sided spectral density of the pressure fluctuations S_p using a Hanning window to reduce spectral leakage and band-averaging using eight fundamental frequencies (bandwidth $\Delta f_b = 1/128$ Hz). Each frequency component j of the resulting discrete pressure spectrum $S_{p,j}$ was then converted

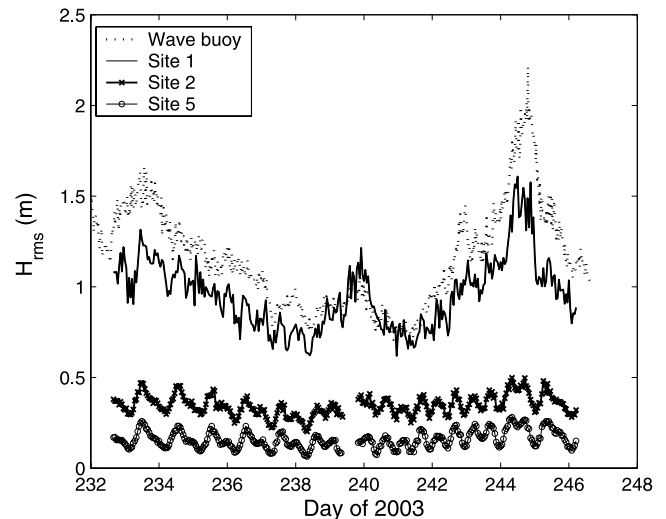


Figure 5. RMS wave height recorded at the offshore wave buoy, site 1 on the fore reef, and sites 2 and 5 on the reef flat.

to a wave spectrum component S_j using linear wave theory according to

$$S_j = \left(\frac{\cosh(k_j h)}{\rho g \cosh(k_j (h - z))} \right)^2 S_{p,j}, \quad (16)$$

where z is the vertical distance of the pressure sensor below the mean surface elevation and k_j is the wave number that is determined by solving the linear dispersion relation

$$\omega_j^2 = g k_j \tanh(k_j h). \quad (17)$$

An analysis of the wave spectra showed that, for all sites, the frequency range 0–0.5 Hz contained greater than 95% of the total energy. As a consequence, in all of the analysis that follows, only wave frequencies up to 0.5 Hz will be considered.

[29] The RMS wave height H_{rms} was calculated for each wave burst by determining the total energy in the wave spectrum, i.e.,

$$H_{rms} = \sqrt{8} \left(\sum_{j=1}^N S_j \Delta f_b \right)^{1/2}, \quad (18)$$

where N is the total number of frequency components. Figure 5 shows H_{rms} calculated during the experiment at the offshore wave buoy, site 1 on the fore reef, and sites 2 and 5 on the reef flat. The average RMS wave height recorded

Table 2. Minimum, Average, and Maximum RMS Wave Height H_{rms} at the Offshore Wave Buoy and Sites 1–5^a

	Wave Buoy	Site 1	Site 2	Site 3	Site 4	Site 5
Minimum	0.70	0.62	0.20	0.15	0.10	0.06
Mean	1.17	0.96	0.35	0.29	0.23	0.17
Maximum	2.21	1.61	0.50	0.47	0.40	0.30

^aWave height is measured in meters.

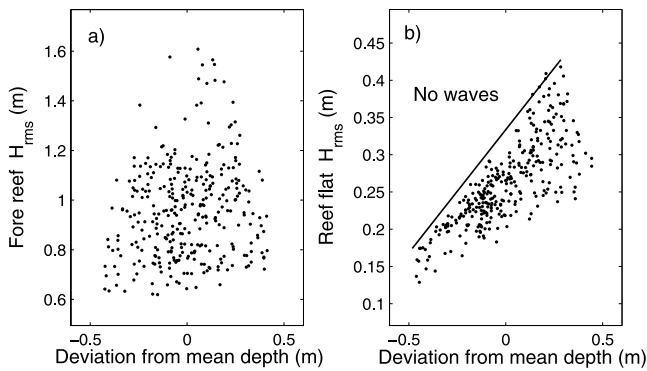


Figure 6. RMS wave height measured on the fore reef and reef flat versus tidal elevation. (a) Fore reef wave height. (b) Reef flat wave height. The solid line indicates the depth-limited wave height.

during the experiment at each site is given in Table 2, along with the minimum and maximum recorded values. Wave heights at site 1 are slightly smaller than the offshore value, although there is good agreement during days 239–242. Figure 4 shows that these days correspond to when the wave direction was more southerly. Therefore the discrepancy appears to be a function of offshore wave direction and may be the result of wave sheltering by Mokapu point located SW of the field site.

[30] A significant decrease in wave height occurred on the fore reef region between sites 1 and 2, due to the combined effects of wave breaking and frictional dissipation. A smaller decrease in wave height occurs between sites 2 and 5 on the reef flat, due to dissipation by bottom friction. The height of waves on the reef flat (sites 2 and 5) falls within a relatively narrow range compared to larger variation in the offshore and fore reef (site 1) values (Figure 5). Wave height on the reef flat is mostly insensitive to the incident wave height because it is controlled by the water depth per equation (1). The wave height on the reef flat is thus controlled by the tidal elevation. This tidal modulation is most apparent in Figure 6, which shows wave height measured on both the fore reef and reef flat plotted as a function of tidal elevation, for all recorded bursts. There is no apparent correlation of the fore reef wave height with water depth. On the reef flat, however, the wave height is a strong function of the water depth because the allowable height of waves on the reef flat increases as the water depth increases.

[31] The wave height on the reef flat is thus a function of both the incident wave height and water depth. Figure 7 shows contours of reef flat wave height plotted as a function of the fore reef wave height (before breaking) and the tidal elevation. During low tides, as the fore reef wave height increases the contours become increasingly vertical implying that the allowable wave height on the reef flat is only a function of the water depth. Alternatively, for cases when the incident waves on the fore reef are small, the contours become increasingly horizontal as the water depth increases, implying that the wave height on the reef flat is now controlled by the incident wave height. Note that the exact shape of the contours in Figure 7 are specific to the Kaneohe reef, and depend on the Kaneohe reef geometry and its wave climate. For shallow reefs that regularly

experience large wave conditions, contours of this type will be mostly vertical as the reef flat wave height will be controlled by the water depth. For deeper reef flats that typically experience small wave conditions, contours will be mostly horizontal as the wave height of the reef flat will not be significantly controlled by the water depth. The Kaneohe Bay barrier reef is clearly an intermediate case where wave height is a function of both tides and offshore wave conditions. Similar contours have been observed using wave height data collected at a site on the Great Barrier Reef by *Hardy and Young* [1996].

4.2. Wave Dissipation

[32] The spatially averaged rate of wave energy dissipation $\langle \epsilon_{\text{total},j} \rangle$, due to both wave breaking and bottom friction, between two arbitrary adjacent sites A and B , can be estimated as a function of the wave frequency component j by discretizing the spectral form of the one-dimensional wave energy equation (equation (2)) as

$$\langle \epsilon_{\text{total},j} \rangle = \langle \epsilon_{f,j} \rangle + \langle \epsilon_{b,j} \rangle \approx \frac{\Delta F_j}{\Delta r} - \Delta R_j \quad (19)$$

$$\Delta r = L_{AB} \cos \theta, \quad (20)$$

where the angled brackets indicate spatial averaging between adjacent sites. Here ΔF_j is the difference in the wave energy flux measured between sites A and B , which can be determined by applying equations (3)–(5), L_{AB} is the direct distance between sites A and B , and θ is the angle formed between the line connecting the two sites and the wave propagation direction. Note that in equation (20), the projected distance Δr is assumed to not be a function of wave frequency, which implies that all waves propagate in the same direction. For waves measured over the reef this was a good assumption, as will be discussed below, since the wave direction is set by the shallow bathymetry.

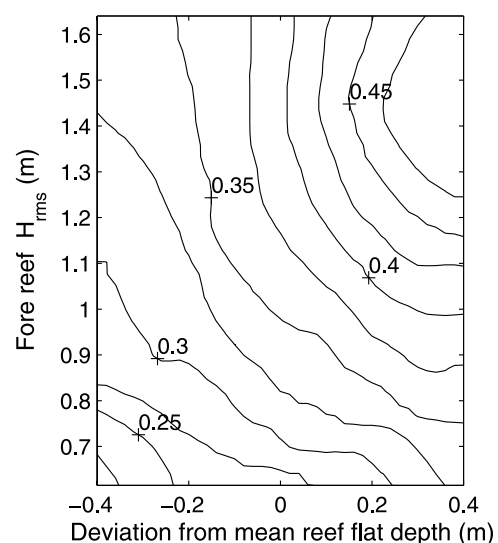


Figure 7. Contours of reef flat RMS wave height measured at site 2 versus fore reef wave height (site 1) and tidal elevation (as represented by deviation from mean reef flat depth). The contour interval is 0.025 m.

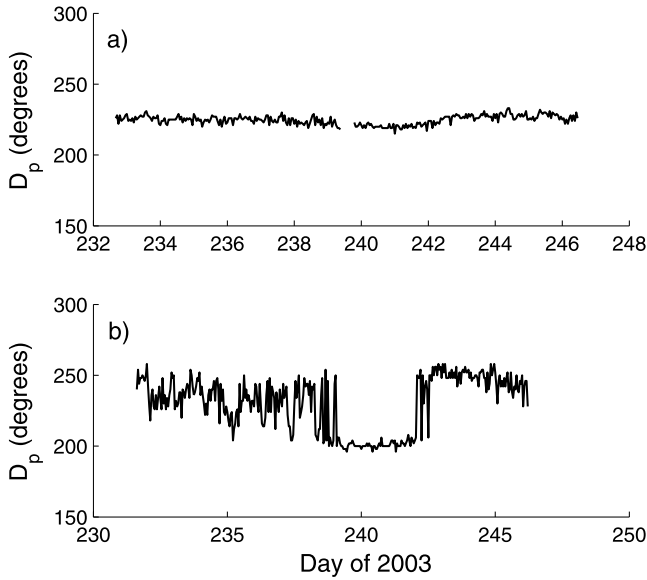


Figure 8. Time series of dominant wave direction D_p measured at (a) site 2 and (b) site 1.

Since equation (19) is based on the one-dimensional wave equation, the term $\Delta R_{r,j}$ is included to account for any apparent decrease in wave energy flux resulting from two-dimensional wave refraction effects. To investigate the magnitude of $\Delta R_{r,j}$, the numerical wave model REF/DIF 1 [Kirby and Dalrymple, 1983] was used to simulate a monochromatic wave field in the study area. To investigate refraction effects, separate simulations were conducted with bottom friction and wave breaking turned off in the model for a range of different incident wave frequencies, and $\Delta R_{r,j}$ was estimated by calculating $\Delta F_j/\Delta r$ between each pair of sites. Results showed that in the worst case $\Delta R_{r,j}/(\Delta F_j/\Delta r) < 0.1$ between each pair of sites on the reef flat (sites 2–5), and hence refraction effects can be neglected since its effect is smaller than the inherent uncertainty in the frictional dissipation estimates discussed below. This estimate of negligible refraction is consistent with previous estimates of refraction made for the same site [Falter et al., 2004].

[33] Wave dissipation $\langle \epsilon_{\text{total},j} \rangle$ was calculated for each frequency component j in each burst using equation (19) between each adjacent pair of sites. Because the linear array of pressure sensors between sites 1 and 5 was not perfectly aligned with the measured wave direction, the Δr term was calculated between each adjacent pair of sites using equation (20). To determine the wave direction θ , the directional wave spectrum was calculated using the pressure and velocity data recorded by the ADVs at site 2 on the reef flat, as well as the ADCP located at site 1, by using the Maximum Entropy Method [Massel, 1996]. The wave direction θ was assumed to be represented by the dominant wave direction D_p that was calculated from the directional spectrum for each burst. Time series of D_p measured at both sites 1 and 2, are shown in Figure 8. The dominant wave direction at site 2 on the reef flat is very constant and averages 225° with very minimal variation of $\pm 2^\circ$. The dominant wave direction measured at site 1 on the fore reef is on average 229° with a larger variation of approximately $\pm 20^\circ$. As expected, the wave direction on the fore reef is more sensitive to

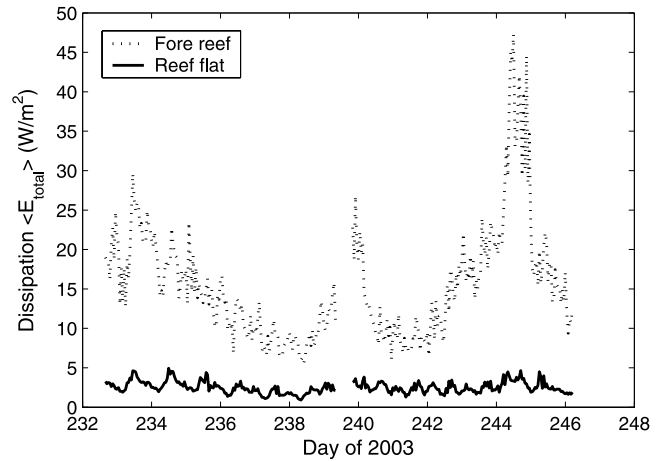


Figure 9. Spatially averaged rate of dissipation $\langle E_{\text{total}} \rangle$ measured on the fore reef and reef flat.

offshore changes in wave direction than on the reef flat since the fore reef is located in deeper water where refraction has less of an influence. For each burst, these measurements of D_p at sites 1 and 2 were used to estimate θ between each pair of sites in order to calculate the projected distance Δr . The projected distance between sites 1 and 2 averaged about 700 m. The projected distance between adjacent sites on the reef flat, each averaged about 100 m.

[34] Dissipation between each pair of sites was calculated for each frequency component in a given burst, by applying equation (19). The total dissipation $\langle E_{\text{total}} \rangle$ for each burst was then calculated by summing the dissipation calculated for each frequency component up to 0.5 Hz, i.e.,

$$\langle E_{\text{total}} \rangle = \sum_{j=1}^N \langle \epsilon_{\text{total},j} \rangle. \quad (21)$$

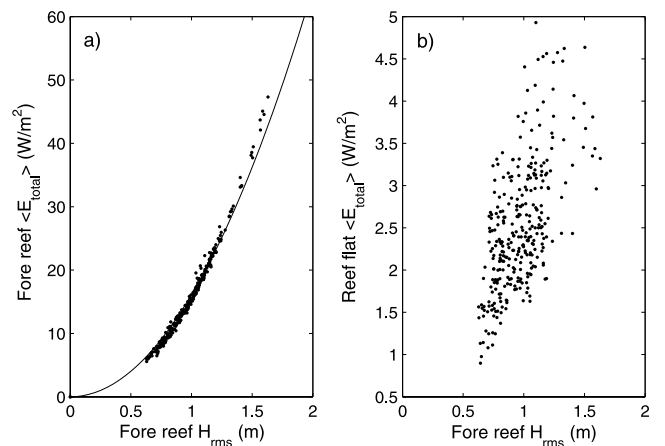


Figure 10. Average rate of dissipation $\langle E_{\text{total}} \rangle$ versus the fore reef wave height (measured at site 1). (a) Dissipation measured on the fore reef between sites 1 and 2, where the solid line indicates a quadratic dependence, obtained by fitting the dissipation data to aH_{rms}^2 , where a is a fitting parameter. (b) Dissipation measured on the reef flat taken as the average of the values measured between sites 2–3, 3–4, and 4–5.

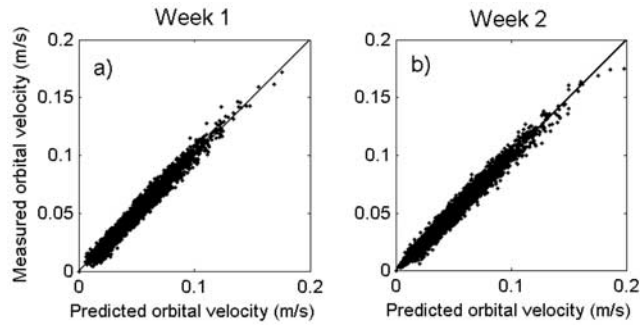


Figure 11. Measured wave orbital velocity $u_{b,j}$ for each frequency component at site 2 versus that predicted from the wave height measurements using linear wave theory for (a) week 1 and (b) week 2 of the experiment.

Figure 9 shows a time series of the total dissipation $\langle E_{\text{total}} \rangle$, which reflects the spatially averaged dissipation rate between the sites. “Fore reef” refers to the dissipation calculated between sites 1 and 2. “Reef flat” refers to the average value calculated for the reef flat sites (between sites 2–3, 3–4 and 4–5) for each burst. The rate of dissipation is generally much higher on the fore reef where dissipation is due to the combined effects of wave breaking and bottom friction.

[35] Figure 10 shows dissipation calculated on the fore reef and reef flat as a function of the incident wave height measured at site 1. Dissipation on the fore reef is highly correlated with the incident wave height. Equation (4) shows that the wave energy flux at each site is proportional to wave height squared. However, compared to the significant variation in the fore reef wave height, the wave height on the reef flat varies minimally (Figure 5) since it is controlled by the water depth per equation (1). The reef flat wave height thus can essentially be treated as a constant, and in this case the total dissipation measured on the fore reef should be approximately proportional to the incident wave height squared. This quadratic dependence is shown as the solid line in Figure 10a. In general, the dissipation measured on the fore reef should not be perfectly quadratic because the wave height on the reef flat is not exactly constant due to the tidal modulation of the water depth.

[36] Similarly, Figure 10b shows reef flat dissipation as a function of the incident wave height measured on the fore reef. In general, reef flat dissipation increases with fore reef wave height although the correlation is smaller than in Figure 10a. Reef flat dissipation is due to frictional dissipation, and according to equation (9) will increase in proportion to the near-bottom wave orbital velocity cubed, and hence proportional to the reef flat wave height cubed. Therefore reef flat dissipation is not well correlated with offshore wave height, since wave height and accordingly frictional dissipation is also a function of the water depth.

4.2.1. Frictional Dissipation on the Reef Flat

[37] Wave dissipation measured on the reef flat between sites 2 and 5 can be used to calculate wave friction parameters for the reef. No wave breaking occurs on the reef flat (i.e., $\epsilon_{b,j} \approx 0$) so the total dissipation measured between sites 2 and 5 can be assumed to be only due to friction. Frictional dissipation is parameterized as a function of the maximum near-bottom horizontal orbital velocity $u_{b,j}$,

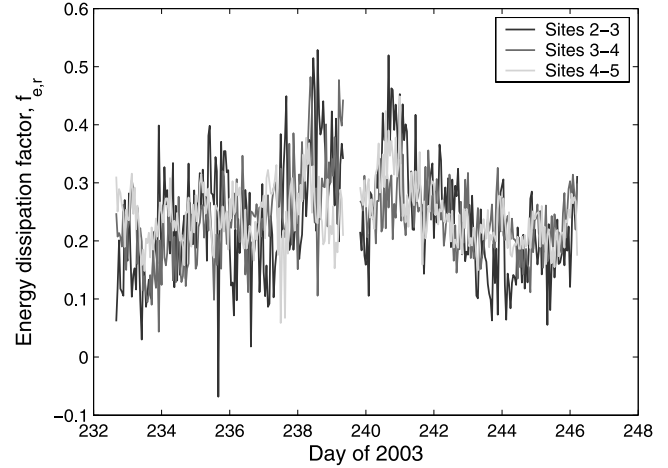


Figure 12. Representative energy dissipation factor $f_{e,r}$ measured between each pair of sites on the reef flat. See color version of this figure in the HTML.

according to equation (9). This velocity was only directly measured at site 2 (see section 3), so at each site $u_{b,j}$ was estimated for each frequency component j using the measured wave spectrum by applying linear wave theory:

$$u_{b,j} = \frac{a_j \omega_j}{\sinh k_j h}, \quad (22)$$

where the wave amplitude component a_j can be determined as $a_j = \sqrt{2S_j \Delta f_b}$. The ADV located at site 2 simultaneously sampled velocity and pressure, allowing a check of the applicability of equation (22), which may break down in shallow depths where nonlinear effects are potentially significant. Figure 11 shows scatter plots of $u_{b,j}$ measured by the lower ADV for each frequency component of each burst, as a function of the corresponding velocity predicted using equation (22), during each week of the experiment. A 1:1 correspondence ($r^2 = 0.98$) is observed over the full range of conditions measured in the experiment, indicating that equation (22) can be applied to obtain accurate estimates of $u_{b,j}$ at each site on the reef flat using the wave height records, similar to findings described by *Guza and Thornton* [1980].

[38] Combining the estimates of $\langle \epsilon_{f,j} \rangle$ and $u_{b,j}$ described above, enables us to calculate the energy dissipation factor $f_{e,j}$ using equation (9) and its representative value $f_{e,r}$ by applying equation (12), between each pair of sites on the reef flat. A time series of $f_{e,r}$ calculated between each pair of sites on the reef flat is shown in Figure 12. In general, $f_{e,r}$ is consistent between the different sites (Table 3), indicating that the frictional properties were independent of where they were measured on the reef flat. The average value of $f_{e,r}$

Table 3. Mean Values of the Representative Frictional Dissipation Parameters Measured Between the Reef Flat Sites

	$u_{bm,r}$, m/s	ω_{r2} , 1/s	$f_{e,r}$	f_w	k_{r2} , m
Sites 2–3	0.30	1.02	0.23	0.28	0.18
Sites 3–4	0.27	1.01	0.24	0.28	0.16
Sites 4–5	0.23	0.98	0.24	0.29	0.15
Mean	0.27	1.00	0.24	0.28	0.16

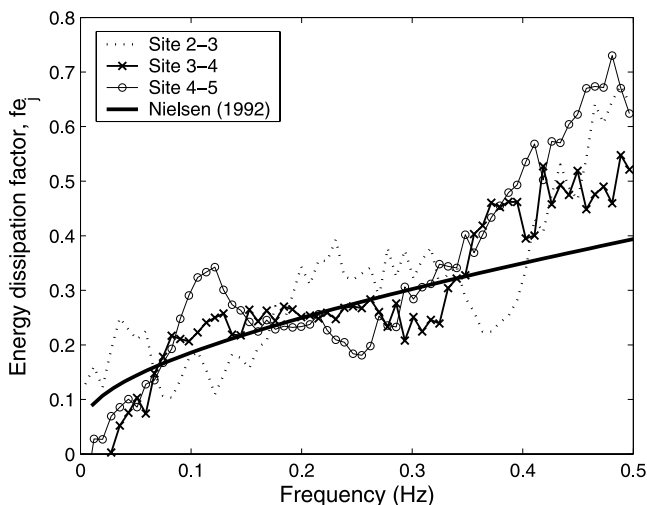


Figure 13. Energy dissipation factor as a function of wave frequency. Measured values are indicated by dotted lines. The solid line represents predicted energy dissipation factor using a constant roughness length $k_w = 0.16$ m.

measured between the reef flat sites during the experiment was $f_{e,r} = 0.24 \pm 0.03$ (Table 3), where the uncertainty is expressed as twice the standard deviation of the mean value. This value $f_{e,r}$ is consistent with previous estimates made on the Kaneohe Bay reef flat ($f_{e,r} = 0.22 \pm 0.03$ [Falter et al., 2004]) and is also comparable to values estimated for other coral reefs such as Ala Moana Reef, Hawaii ($f_{e,r} = 0.28 \pm 0.25$ [Gerritsen, 1981]) and John Brewer Reef, Great Barrier Reef ($f_{e,r} = 0.15 \pm 0.04$ [Nelson, 1996]).

4.2.2. Hydraulic Roughness

[39] Using the measured values for $u_{b,r}$, ω_r and $f_{e,r}$, the wave friction factor $f_{w,r}$ and hydraulic roughness length k_w can be determined using equations (13)–(15). The average values of $f_{w,r}$ and k_w , calculated between each pair of sites on the reef flat are shown in Table 3. Note that $f_{w,r}$ is approximately 20% larger than $f_{e,r}$ which is due to the assumed phase lag ϕ_r between the maximum shear stress and the maximum near-bottom velocity. It should be emphasized that the average $f_{w,r}$ calculated for the duration of the experiment was $f_{w,r} = 0.28 \pm 0.04$, which is 30 times larger than a typical value of 0.01 cited for flat sandy bottoms [e.g., Thornton and Guza, 1983]. Coral reef surfaces are thus highly efficient at dissipating wave energy by bottom friction due to the large bottom roughness produced by reef organisms. The hydraulic roughness length k_w (calculated using equation (13)) does not vary significantly between locations on the reef flat, and has an average value $k_w = 0.16 \pm 0.03$ m for this experiment, as shown in Table 3.

[40] An advantage of the spectral wave friction model of Madsen [1994] is that it can be used to investigate how wave energy is dissipated among the different frequency components. For each burst, $\langle \epsilon_{f,j} \rangle$ was calculated for each frequency component, and equation (9) was applied to determine the energy dissipation factor $f_{e,j}$ as a function of wave frequency. The energy dissipation factor $f_{e,j}$, ensemble averaged over all bursts during the 2 week experiment, is shown in Figure 13. There is a general trend of increasing energy dissipation factor as the wave frequency increases, which is consistent between the different pairs of sites. In

laboratory experiments, Mathisen and Madsen [1999] showed that a single hydraulic roughness length k_w works well to predict how the energy dissipation factor varies as a function of wave frequency. The predicted shape of $f_{e,j}$ using equation (13) and the measured value $k_w = 0.16$ m held constant, is plotted as a solid line in Figure 13. The model prediction agrees very well with the form of $f_{e,j}$ observed in the experiments, and only deviates significantly from the observed measurements for frequencies greater than about 0.4 Hz. At higher frequencies (>0.4 Hz), the measured energy dissipation factor is larger than that predicted using the model. It is possible that this deviation is due to nonlinear energy transfer, as discussed below. Another, likely possibility, is that at high wave frequencies the ratio $u_{b,r}/(k_w\omega_j)$ becomes order one which implies that the magnitude of the near-bed wave orbital excursion length is comparable to the roughness length scale. When this is the case, the wave friction factor becomes dependent on the bottom roughness geometry and wave friction formulas are likely to break down. As a consequence, many friction models suggest a maximum applicability limit based on $u_{b,r}/(k_w\omega_j)$ [e.g., Madsen, 1994], but no upper limit is specifically stated for the Nielsen [1992] formula. Regardless of the discrepancy at high frequencies, the bulk of the total wave energy is located in the frequency range 0.1–0.25 Hz and within this range the agreement is excellent. It should be emphasized that the spectral friction model neglects the potential transfer of energy among the different frequency components due to nonlinear interactions, which could contaminate the dissipation estimates. As there is no simple method to analytically determine this rate of nonlinear energy transfer [Hamm et al., 1993], the specific effect of nonlinear interactions at this site is unknown. Nevertheless, the fact that the rates of dissipation predicted using the Madsen et al. [1988] model agree so well with our observations may suggest that the rate of nonlinear energy transfer on this flat surface is negligible over these short distances compared to the high rate of frictional dissipation on the reef.

[41] In order to predict rates of frictional dissipation at arbitrary field sites, values for parameters in the friction models must be specified. Estimates of the hydrodynamic

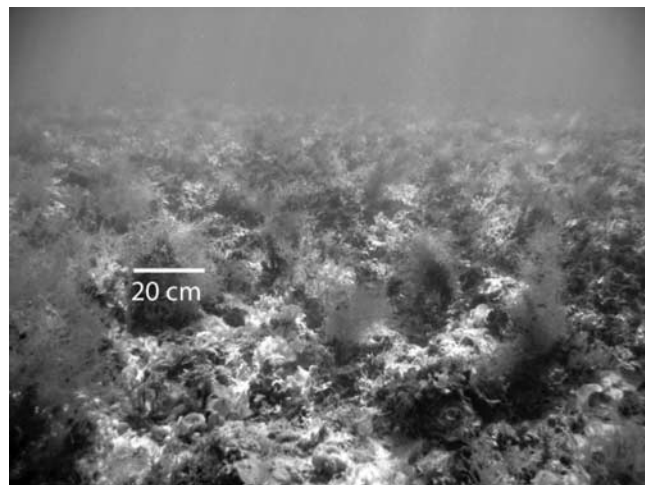


Figure 14. Photograph taken on the reef flat between sites 2 and 3. See color version of this figure in the HTML.

parameters in these models are simple as these are defined by the incident wave field. However, a hydraulic roughness length k_w must also be specified which may be challenging since the bottom roughness characteristics depend on the particular field site. In principle, k_w can be determined from wave attenuation measurements as we have done here, but in practice it would be preferable to specify k_w based on the physical roughness of the reef, which could potentially be obtained by doing bottom roughness surveys.

[42] A major question then is, how well does k_w obtained from the wave friction estimates relate to actual measurements of the bottom roughness. Figure 14 shows a photo of the reef flat taken between sites 2 and 3. The reef flat is composed of a hard limestone base which is covered by a variety of benthic organisms, including various species of algae and coral [Falter *et al.*, 2004]. To measure the bottom roughness, surveys were conducted at 14 random locations distributed across the reef flat study area (between sites 2 through 5). At each survey location a roughness profiler, similar to the apparatus described by McCormick [1994] and detailed by V. Nunes and G. Pawlak (manuscript in preparation, 2005), was used to measure the height of the roughness in the cross-reef direction in 5 cm intervals along a 3 m transect to a vertical resolution of ± 2 mm. Roughness along each transect was characterized by the standard deviation of the substratum heights σ_r which is equivalent to the RMS roughness amplitude. Values of σ_r measured for the 14 transects averaged 3.6 cm and ranged from 2.0 to 4.9 cm. The variation in the measured roughness between the survey sites was surprisingly small, suggesting that the reef flat roughness is mostly homogeneous within the study area. In order to compare the hydraulic roughness k_w with the measured roughness, the same definition of k_w in Nielsen's [1992] friction formula (equation (13)) must be used. This equation was derived from laboratory experiments using nonmovable three-dimensional roughness (e.g., fixed sand, pebbles, gravel, etc.) where the hydraulic roughness was assigned a value of $k_w = 2D$ based on the grain diameter D [Nielsen, 1992]. The measured RMS roughness height is $2\sigma_r$ (twice the roughness amplitude) and to an approximation it is reasonable to assume that $D \approx 2\sigma_r$. Hence to specify a value of k_w consistent with its definition in equation (13), the expression

$$k_w \approx 4\sigma_r \quad (23)$$

can be used to an approximation. Applying equation (23) to the roughness measurements produces an average value of $k_w = 14$ cm. This value is remarkably similar to the hydraulic roughness obtained using equation (13) with the bottom friction measurements ($k_w = 16 \pm 3$ cm), and is most importantly of the correct order of magnitude, suggesting that it may be possible to predict frictional dissipation on coral reefs by making small-scale surveys of the bottom roughness. Although these results show great promise, it must be emphasized that this comparison has only been applied using this data set and to verify whether this approach is consistently valid on coral reefs and not coincidental, similar data collected on other reefs is needed.

[43] Finally, it should be noted that the hydraulic roughness k_w in equation (23) has been characterized by a single length scale based on the RMS roughness height. Yet,

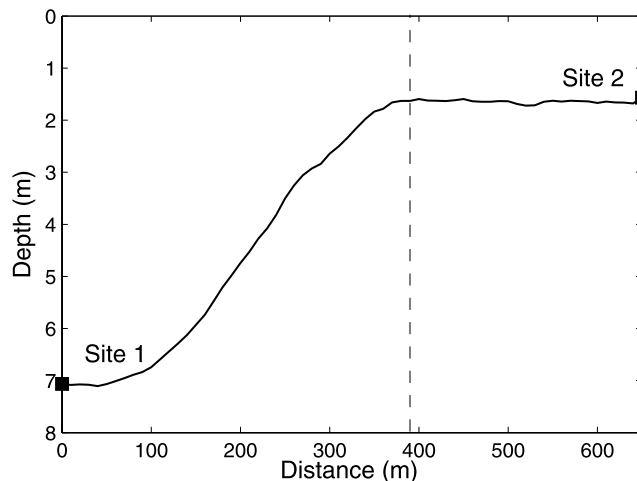


Figure 15. Water depth profile, as referenced to the mean tidal elevation, between sites 1 and 2. The vertical dashed line indicates the approximate location of the reef crest.

studies have shown that the hydraulic roughness can be a function of not only the height of the roughness but also the roughness element spacing and distribution. The hydraulic roughness associated with a two-dimensional vortex ripple, for example, is known to be a function of both the ripple height and its wavelength [Nielsen, 1992]. Laboratory experiments have also shown that inhomogeneities in roughness can establish residual circulations that can alter dissipation [Pawlak and MacCready, 2002]. The Kaneohe reef flat, however, does not appear to have organized two-dimensional spatial structure. Having formed from eroded limestone, benthic organisms and coral rubble, the reef flat roughness is three-dimensional in nature and is thus well approximated by the three-dimensional, "sand-grain" roughness used in laboratory experiments to derive the Nielsen [1992] friction formula given in equation (13).

4.2.3. Wave Breaking Dissipation on the Fore Reef

[44] The direct measure of wave breaking dissipation in the field environment is difficult. For our experiment, wave breaking occurred in the surf zone between sites 1 and 2. Between these sites, however, frictional dissipation also occurs which prevents us from directly measuring the effects of breaking alone. In order to investigate the contribution of wave breaking to the total dissipation measured between sites 1 and 2, a simple one-dimensional numerical model was implemented. The model follows the approach described by Thornton and Guza [1983], which is based on solving the wave energy equation in equation (2). In their approach, the wave energy equation is integrated such that the total energy in the spectrum is modeled, not the individual contributions of the frequency components, i.e.,

$$\frac{\partial F}{\partial x} = -E_b - E_f, \quad (24)$$

where F represents the total (sum over all frequencies) wave energy flux, E_b represents the total rate of wave breaking dissipation, and E_f is the total rate of frictional dissipation. Equation (24) is numerically integrated from site 1 to site 2 using a forward differencing scheme. A grid convergence test was done and a step size of 1 m was found to be

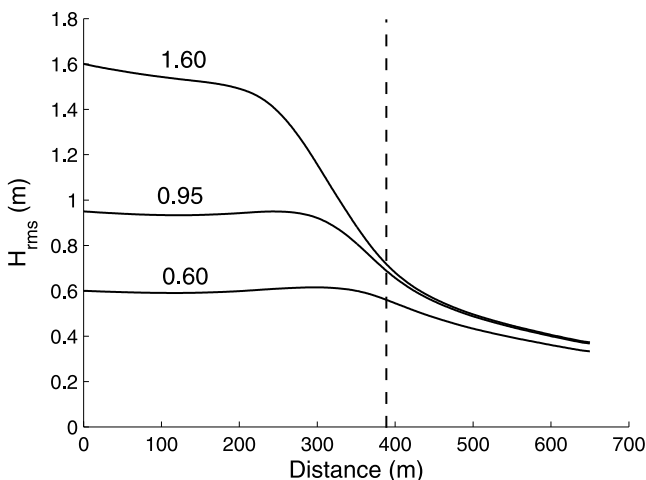
Table 4. Results From the Wave Transformation Model Calculations

Parameter	Run 1	Run 2	Run 3
H_{rms} (site 1), m	0.60	0.95	1.60
H_{rms} (site 2), m	0.33	0.37	0.37
$\langle E_f \rangle$, W/m^2	2.91	5.35	9.24
$\langle E_b \rangle$, W/m^2	0.74	4.94	21.89
$\langle E_{\text{total}} \rangle$, W/m^2	3.66	10.29	31.13
$\langle E_f \rangle / \langle E_b \rangle$	3.92	1.10	0.42
$\Sigma E_b / \Sigma E_{\text{total}}$	0.16	0.44	0.68
$\Sigma E_f / \Sigma E_{\text{total}}$	0.84	0.56	0.32

adequate, since further reducing the step size had a negligible influence on the results. Figure 15 shows the bathymetry profile along a line between sites 1 and 2, which was used as an input to the model.

[45] Frictional dissipation E_f was parameterized using the representative hydraulic roughness $k_w = 0.16$ m measured on the reef flat. The bottom roughness between sites 1 and 2 is believed to be comparable to that measured on the reef flat, since it is covered with similar reef organisms. To parameterize wave breaking dissipation, the mild bed slope model of *Thornton and Guza* [1983] was used as given in equation (6). The applicability of this model to coral reefs has been questioned by *Massel and Gourlay* [2000], since it may not accurately predict wave breaking on very steep coral reef slopes, however, the barrier reef at Kaneohe Bay is unusually wide and consequently has a relatively mild slope. Between sites 1 and 2, the fore reef has a slope of 1:50 which is the same slope as the sandy beach site that was used for the original model calibration [*Thornton and Guza*, 1983]. The empirical constants in the breaking dissipation model, equation (6), were set to $\gamma = 0.5$ and $B = 1$ which represent standard values cited in the literature.

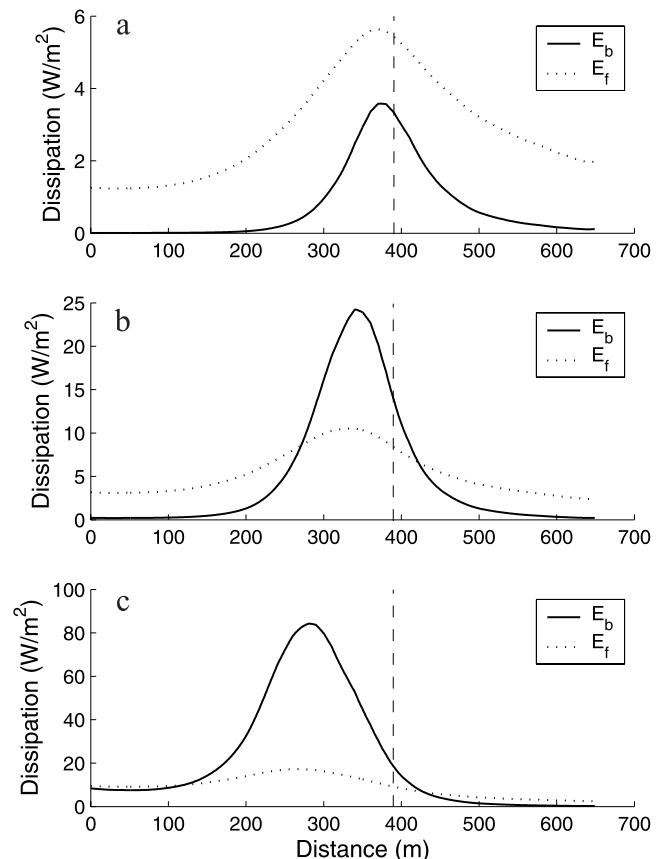
[46] The model was run using the mean tidal elevation and a constant wave period of 7.5 s, which represents the average offshore peak period T_p recorded during the experiment (see Figure 4). The RMS wave height was initialized at site 1 using the range of values shown in Table 4, and

**Figure 16.** RMS wave height predicted using the numerical model for incident wave heights of 0.60 m, 0.95 m, and 1.60 m. The location of the reef crest is indicated by the dashed line.

equation (24) was integrated along the line connecting sites 1 and 2. The initial wave heights at site 1 were chosen to represent three different conditions: (1) the minimum recorded wave height measured at site 1 during the experiment, $H_{\text{rms}} = 0.60$ m, (2) the mean wave height, $H_{\text{rms}} = 0.95$ m, and (3) the maximum recorded wave height, $H_{\text{rms}} = 1.60$ m.

[47] Figure 16 shows the computed wave transformation as the waves propagate from site 1 to 2, for the range of wave conditions encountered in the experiments. In general, there is a monotonic decrease in wave height as wave energy is dissipated due to breaking and frictional dissipation, although there is a slight increase in wave height on the fore reef slope for small wave conditions, which is attributed to shoaling effects. A rapid decrease in wave height occurs about 100 m seaward of the reef crest. The final predicted wave height at site 2 varied between 0.33 and 0.37 m, which is consistent with the mean value recorded at site 2 during the experiment of 0.35 m (see Table 2). The model clearly shows that the wave height on the reef flat is controlled by the water depth. Despite the considerable variation in the wave height at site 1, for the fixed tidal elevation used in the model the wave height at site 2 is approximately constant near 0.35 m for all incident wave conditions, as shown in Table 4.

[48] The numerical model can be used to determine rates of dissipation between site 1 and 2 and how it is partitioned

**Figure 17.** Profiles of dissipation calculated using the model, where E_b is the rate of breaking dissipation and E_f is the rate of frictional dissipation for incident RMS wave heights of (a) 0.60 m, (b) 0.95 m, and (c) 1.60 m.

between wave breaking and bottom friction. Table 4 shows the spatially averaged total rate of dissipation $\langle E_{\text{total}} \rangle = \langle E_b \rangle + \langle E_f \rangle$, due to the sum of wave breaking and bottom friction, for the range of wave conditions encountered in the experiment. Comparison with the measured rate of dissipation in Figure 9 shows that these values agree fairly well with the observations, indicating that this simple model accurately represents dissipation on the fore reef.

[49] Figure 17 shows the individual contribution of wave breaking and bottom friction plotted as a function of distance from site 1. Both wave breaking and bottom friction dissipation rates peak slightly behind the reef crest for all wave conditions. However, the relative contribution of wave breaking and bottom friction is a strong function of the incident wave conditions. For small wave conditions ($H_{\text{rms}} = 0.60$ m) the fore reef region is dominated by frictional dissipation and Table 4 shows that the average rate of frictional dissipation $\langle E_f \rangle$ in this region is about 4 times larger than wave breaking dissipation $\langle E_b \rangle$. For the average wave conditions ($H_{\text{rms}} = 0.95$ m) the average rate of frictional dissipation approximately equals the rate of wave breaking dissipation although the magnitude of the peak for breaking dissipation is higher within the surf zone. For the largest wave conditions encountered during the experiment ($H_{\text{rms}} = 1.60$ m) the average rate of dissipation due to bottom friction is still comparable to that due to breaking. Thus despite the presence of the surf zone, the frictional contribution to the total dissipation measured on the fore reef is surprisingly important for the full range of wave conditions encountered in this experiment.

[50] Finally, results from the model can be used to estimate how the overall incident wave energy dissipated by the reef is partitioned between wave breaking and bottom friction. The total wave energy dissipated by the reef is denoted ΣE_{total} , which is the sum of the total wave breaking ΣE_b and total frictional ΣE_f contributions. To an approximation it will be assumed that the total energy incident on the reef is represented by the energy flux F_1 measured at site 1, and that all of this energy is dissipated in some form by the reef in the region onshore of this site, i.e., $\Sigma E_{\text{total}} \approx F_1$. This value will be slightly smaller than the actual total energy dissipated, due to the fact that some unaccounted for energy is dissipated offshore of site 1 by friction, but importantly not by wave breaking. Since all wave breaking occurs between sites 1 and 2, the model results above can be used to calculate the total wave energy dissipated by breaking on the reef ΣE_b . The total energy dissipated by friction is simply the difference between the total dissipation and wave breaking dissipation, i.e., $\Sigma E_f = \Sigma E_{\text{total}} - \Sigma E_b$. Hence the partitioning of total dissipation between wave breaking and bottom friction can be estimated from the model calculations. Table 4 shows the fraction of wave breaking and frictional dissipation with respect to total dissipation for the three wave conditions used in the model. For small waves ($H_{\text{rms}} = 0.60$ m) greater than 80% of the total incident energy is dissipated by friction and for average conditions ($H_{\text{rms}} = 0.95$ m) approximately 60% is dissipated by friction. Only for large wave conditions ($H_{\text{rms}} = 1.60$ m) does wave breaking dominate, but even then frictional dissipation is still important, contributing greater than 30% to the total. Hence frictional dissipation is very important on this reef, and

since additional frictional dissipation occurring offshore of site 1 is not included in these calculations, it is safe to assume that on average a majority of wave energy incident on the Kaneohe Bay barrier reef is dissipated by bottom friction.

5. Summary and Conclusions

[51] Results from a 2 week experiment on the Kaneohe Bay barrier reef show that for typical wave conditions, a majority of the incident wave energy is dissipated by bottom friction, and that wave breaking is of lesser importance. This is in contrast to observations made on sandy beach sites [e.g., *Thornton and Guza*, 1983] and some assumptions about dissipation on other coral reefs [e.g., *Young*, 1989; *Gourlay*, 1994; *Massel and Gourlay*, 2000], where wave breaking is assumed to dominate and bottom friction makes a smaller contribution. A major morphological function of barrier reefs is to impede the transmission of wave energy, acting as a break water, and hence to predict wave attenuation by reefs, an accurate parameterization of all dissipation processes is needed. Frictional dissipation is often expected to be of prime importance on coral reefs and hence its accurate parameterization must be incorporated into wave models of these sites.

[52] The spectral wave friction model of *Madsen et al.* [1988] appears to accurately describe rates of frictional dissipation measured on the reef flat. Moreover, the use of a single hydraulic roughness seems to describe the observed variation in the dissipation rates among the different frequency components, similar to findings in previous studies conducted in smaller-scale laboratory flumes [*Mathisen and Madsen*, 1999]. Results from the bottom roughness survey conducted on the reef flat indicate that the measured roughness compares well to the hydraulic roughness obtained with the frictional dissipation measurements using *Nielsen's* [1992] wave friction formula. This suggests that it may be possible to characterize frictional dissipation on other reefs from local measurements of bottom roughness and wave kinematics, rather than derived from large-scale observations of wave transformation. Such an approach would be more useful in reef environments where the wave fields are generally more complex and/or the effect of bottom friction is overshadowed by other wave-transforming processes such as refraction, diffraction, and breaking.

Notation

$\langle \rangle$	operator indicating spatial average value between sites.
a	wave amplitude.
A_b	near-bed wave orbital excursion amplitude.
B	empirical wave breaking constant.
C_g	group velocity.
D	grain diameter.
D_p	dominant wave direction.
E	wave energy density.
E_b	total rate of breaking dissipation summed over all frequency components.
E_f	total rate of frictional dissipation summed over all frequency components.
E_{total}	sum of E_b and E_f .
f_e	wave energy dissipation factor.

- f_p peak wave frequency.
 f_w wave friction factor.
 F wave energy flux.
 F_1 wave energy flux measured at site 1.
 g gravitational acceleration.
 h water depth.
 H_{rms} root-mean-squared wave height.
 k wave number.
 k_w hydraulic roughness length.
 L_{AB} direct distance between adjacent sites.
 N number of discrete frequency components.
 S wave spectrum.
 S_p pressure spectrum.
 T_p peak wave period.
 u_b near-bed maximum horizontal wave orbital velocity.
 U current velocity.
 x cross-reef direction.
 z vertical distance measured below the mean free surface level.
 γ critical wave breaking ratio.
 Δ_R difference in energy flux between sites due to refraction.
 Δf_b frequency bandwidth.
 ΔF difference in wave energy flux measured between sites.
 Δr projected distance between sites in the wave direction.
 ϵ_b rate of breaking dissipation.
 ϵ_f rate of frictional dissipation.
 ϵ_{total} sum of ϵ_b and ϵ_f .
 θ angle between wave direction and adjacent sites.
 ρ density of seawater.
 σ_r root-mean-squared bottom roughness amplitude.
 ΣE_b total incident wave energy dissipated by breaking on the reef.
 ΣE_f total incident wave energy dissipated by friction on the reef.
 ΣE_{total} sum of ΣE_b and ΣE_f .
 τ_w wave-induced bed shear stress.
 ϕ phase difference between bottom stress and orbital velocity.
 ω radian wave frequency.
- Subscripts**
 j frequency component j .
 r representative parameter.

[53] **Acknowledgments.** The authors are grateful to Jim Fleming for assisting with the experimental setup and instrument deployment. We also thank Vasco Nunes for offering the use of his roughness profiler to conduct the bottom roughness surveys and Jerome Aucan and Mark Merrifield at the UH Sea Level Center for providing the offshore wave buoy data. Landsat 7 ETM+ image of Kaneohe Bay in Figure 2 is distributed by the Land Processes Distributed Active Archive Center (LP DAAC), located at the U.S. Geological Survey's EROS Data Center (<http://LPDAAC.usgs.gov>). Image processed by Eric Hochberg. This work was supported by the National Science Foundation under grant OCE-0117859.

References

- Atkinson, M. J., and R. W. Bilger (1992), Effects of water velocity on Phosphate uptake in coral reef-flat communities, *Limnol. Oceanogr.*, *37*, 273–279.

- Baird, M. E., and M. J. Atkinson (1997), Measurement and prediction of mass transfer to experimental coral reef communities, *Limnol. Oceanogr.*, *42*, 1685–1693.
- Battjes, J. (1974), Surf similarity, in *Proceedings of the 14th Coastal Engineering Conference*, pp. 466–480, Am. Soc. of Civ. Eng., Reston, Va.
- Battjes, J., and J. Janssen (1979), Energy loss and set-up due to breaking of random waves, in *Proceedings of the 16th Coastal Engineering Conference*, vol. 1, pp. 563–587, Am. Soc. of Civ. Eng., Reston, Va.
- Brander, R. W., P. S. Kench, and D. Hart (2004), Spatial and temporal variations in wave characteristics across a reef platform, Warraber Island, Torres Strait, Australia, *Mar. Geol.*, *207*, 169–184.
- Chawla, A., H. T. Ozkan-Haller, and J. T. Kirby (1998), Spectral model for wave transformation and breaking over irregular bathymetry, *J. Waterw. Port Coastal Ocean Eng.*, *124*, 189–198.
- Dally, W. R., R. G. Dean, and R. A. Dalrymple (1985), Wave height variation across beaches of arbitrary profile, *J. Geophys. Res.*, *90*, 1917–1927.
- Dean, R., and R. Dalrymple (1991), *Water Wave Mechanics for Engineers and Scientists*, *Adv. Ser. Ocean Eng.*, vol. 2, World Sci., Hackensack, N. J.
- Dollar, S. J. (1982), Wave stress and coral community structure in Hawaii, *Coral Reefs*, *1*, 71–81.
- Dollar, S. J., and G. W. Tribble (1993), Recurrent storm disturbance and recovery—A long-term study of coral communities in Hawaii, *Coral Reefs*, *12*, 223–233.
- Falter, J. L., M. J. Atkinson, and M. Merrifield (2004), Mass transfer limitation of nutrient uptake by a wave-dominated reef flat community, *Limnol. Oceanogr.*, *49*, 1820–1831.
- Gerritsen, F. (1981), Wave attenuation and wave set-up on a coastal reef, *Tech. Rep. 48*, Look Lab. Univ. Hawaii, Honolulu.
- Gourlay, M. R. (1994), Wave transformation on a coral-reef, *Coastal Eng.*, *23*, 17–42.
- Grigg, R. W. (1998), Holocene coral reef accretion in Hawaii: A function of wave exposure and sea level history, *Coral Reefs*, *17*, 263–272.
- Guza, R. T., and E. B. Thornton (1980), Local and shoaled comparisons of sea surface elevations, pressures, and velocities, *J. Geophys. Res.*, *85*, 1524–1530.
- Hamm, L., P. Madsen, and D. Peregrine (1993), Wave transformation in the nearshore zone: A review, *Coastal Eng.*, *21*, 5–39.
- Hardy, T. A., and I. R. Young (1996), Field study of wave attenuation on an offshore coral reef, *J. Geophys. Res.*, *101*, 14,311–14,326.
- Hasselmann, K. (1962), On the non-linear energy transfer in a gravity-wave spectrum. 1. General theory, *J. Fluid Mech.*, *12*, 481–500.
- Hearn, C. J. (1999), Wave-breaking hydrodynamics within coral reef systems and the effect of changing relative sea level, *J. Geophys. Res.*, *104*, 30,007–30,019.
- Hearn, C. J., M. J. Atkinson, and J. L. Falter (2001), A physical derivation of nutrient-uptake rates in coral reefs: Effects of roughness and waves, *Coral Reefs*, *20*, 347–356.
- Jonsson, I. (1966), Wave boundary layers and friction factors, in *Tenth Conference on Coastal Engineering*, vol. 1, Am. Soc. of Civ. Eng., Reston, Va.
- Kajiura, K. (1968), A model of the bottom boundary layer in water waves, *Bull. Earthquake Res. Inst.*, *46*, 75–126.
- Kirby, J. T., and R. A. Dalrymple (1983), A parabolic equation for the combined refraction diffraction of stokes waves by mildly varying topography, *J. Fluid Mech.*, *136*, 453–466.
- Komar, P. (1998), *Beach Processes and Sedimentation*, 2nd ed., Prentice-Hall, Upper Saddle River, N. J.
- Kraines, S. B., A. Suzuki, T. Yanagi, M. Isobe, X. Y. Guo, and H. Komiyama (1999), Rapid water exchange between the lagoon and the open ocean at Majuro Atoll due to wind, waves, and tide, *J. Geophys. Res.*, *104*, 15,635–15,653.
- Lee, T., and K. P. Black (1979), The energy spectra of surf waves on a coral reef, in *Proceedings of the 16th Coastal Engineering Conference*, vol. 1, pp. 588–608, Am. Soc. of Civ. Eng., Reston, Va.
- Longuet-Higgins, M. S., and R. W. Stewart (1962), Radiation stress and mass transport in gravity waves, with application to surf beats, *J. Fluid Mech.*, *13*, 481–504.
- Lugo-Fernandez, A., H. H. Roberts, and J. N. Suhayda (1998a), Wave transformations across a Caribbean fringing-barrier coral reef, *Cont. Shelf Res.*, *18*, 1099–1124.
- Lugo-Fernandez, A., H. H. Roberts, and W. J. Wiseman (1998b), Tide effects on wave attenuation and wave set-up on a Caribbean coral reef, *Estuarine Coastal Shelf Sci.*, *47*, 385–393.
- Madsen, O. S. (1994), Spectral wave-current bottom boundary layer flows, in *Coastal Engineering 1994: Proceedings of the Twenty-Fourth International Conference*, edited by B. L. Edge, pp. 623–634, Am. Soc. of Civ. Eng., Reston, Va.

- Madsen, O., Y.-K. Poon, and H. Graber (1988), Spectral wave attenuation by bottom friction: Theory, in *Coastal Engineering 1998*, vol. 1, pp. 492–504, Am. Soc. of Civ. Eng., Reston, Va.
- Massel, S. (1996), *Ocean Surface Waves: Their Physics and Prediction*, Adv. Ser. Ocean Eng., vol. 11, World Sci., Hackensack, N. J.
- Massel, S. R., and M. R. Gourlay (2000), On the modelling of wave breaking and set-up on coral reefs, *Coastal Eng.*, 39, 1–27.
- Mathisen, P. P., and O. S. Madsen (1999), Waves and currents over a fixed rippled bed: 3. Bottom and apparent roughness for spectral waves and currents, *J. Geophys. Res.*, 104, 18,447–18,461.
- McCormick, M. (1994), Comparison of field methods for measuring surface topography and their associations with a tropical reef assemblage, *Mar. Ecol. Prog. Ser.*, 112, 87–96.
- Nelson, R. C. (1996), Hydraulic roughness of coral reef platforms, *Appl. Ocean Res.*, 18, 265–274.
- Nielsen, P. (1992), *Coastal Bottom Boundary Layers and Sediment Transport*, Adv. Ser. Ocean Eng., vol. 4, World Sci., Hackensack, N. J.
- Pawlak, G., and P. MacCready (2002), Oscillatory flow across an irregular boundary, *J. Geophys. Res.*, 107(C5), 3036, doi:10.1029/2000JC000596.
- Putman, J., and J. Johnson (1949), The dissipation of wave energy by bottom friction, *Eos Trans. AGU*, 30, 67–74.
- Swart, D. (1974), Offshore sediment transport and equilibrium beach profiles, *Tech. Rep. 131*, Delft Hydraul. Lab., Netherlands.
- Symonds, G., K. P. Black, and I. R. Young (1995), Wave-driven flow over shallow reefs, *J. Geophys. Res.*, 100, 2639–2648.
- Tartinville, B., and J. Rancher (2000), Wave-induced flow over Mururoa atoll reef, *J. Coastal Res.*, 16, 776–781.
- Thomas, F. I. M., and M. J. Atkinson (1997), Ammonium uptake by coral reefs: Effects of water velocity and surface roughness on mass transfer, *Limnol. Oceanogr.*, 42, 81–88.
- Thornton, E. B., and R. T. Guza (1982), Energy saturation and phase speeds measured on a natural beach, *J. Geophys. Res.*, 87, 9499–9508.
- Thornton, E. B., and R. T. Guza (1983), Transformation of wave height distribution, *J. Geophys. Res.*, 88, 5925–5938.
- Wiens, H. (1962), *Atoll Environment and Ecology*, Yale Univ. Press, New Haven, Conn.
- Young, I. R. (1989), Wave transformation over coral reefs, *J. Geophys. Res.*, 94, 9779–9789.

M. J. Atkinson and J. L. Falter, Hawaii Institute of Marine Biology, University of Hawaii, 46-007 Lilipuna Road, Kaneohe, HI 96744, USA. (mja@hawaii.edu; falter@hawaii.edu)

M. D. Bandet and G. Pawlak, Department of Oceans and Resources Engineering, Holmes Hall 404, University of Hawaii, 2540 Dole Street, Honolulu, HI 96822, USA. (marionb@hawaii.edu; gpawlak@oe.soest.hawaii.edu)

J. R. Koseff, R. J. Lowe, and S. G. Monismith, Environmental Fluid Mechanics Laboratory, Stanford University, Stanford, CA 94305-4020, USA. (koseff@stanford.edu; rlowe@stanford.edu; monismith@stanford.edu)